Report

GETEC project

Title : GETEC project

Authors : Juliana G. R. de Carvalho, Luewton L F Agostinho, Alexander Finnegan, Janneke Dickhout

Date : December 2, 2024

Code :

Version : 1

Status : draft

Mailing list :

Copy to :

Classification : confidential

Contents

1 WP3 Overview

EXAMPLE CITATION

(Carrasco-Munoz et al., 2022).

1.1 Objectives

Bases on the signed proposal, ...

1.2 Timeline of Executed Tasks

1.3 Conventions

Throughout this section, we'll refer multiple times to physical variables of the system. Figure 1 shows the variable conventions we'll use in this text.

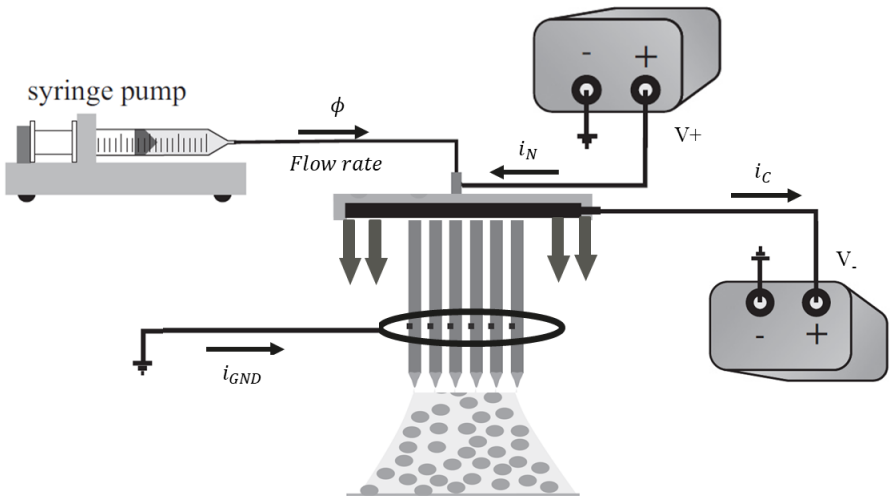

Figure 1. Variable conventions and nomenclature. SOURCE - ADAPTED FROM VERDOOLD

As shown in Figure 1, we have

- i_N: current flowing from the positive high voltage source to the nozzles
- i_C: current flowing from the crown to the negative high voltage source
- i_{GND}: current flowing from the ground to the ring
- ϕ: flow rate of the syringe pump

- V_+: voltage of the positive high voltage
- V_-: voltage of the negative high voltage

The direction of the currents was chosen as shown in Figure 1 to ensure they are always positve in the measurements, faciliting the analysis.

2 First Approach: PID Controller

2.1 Time Response Analysis

Before developing a proof-of-concept PID controller for the multinozzle, we first need to understad the time resonse of system to changes in the input.

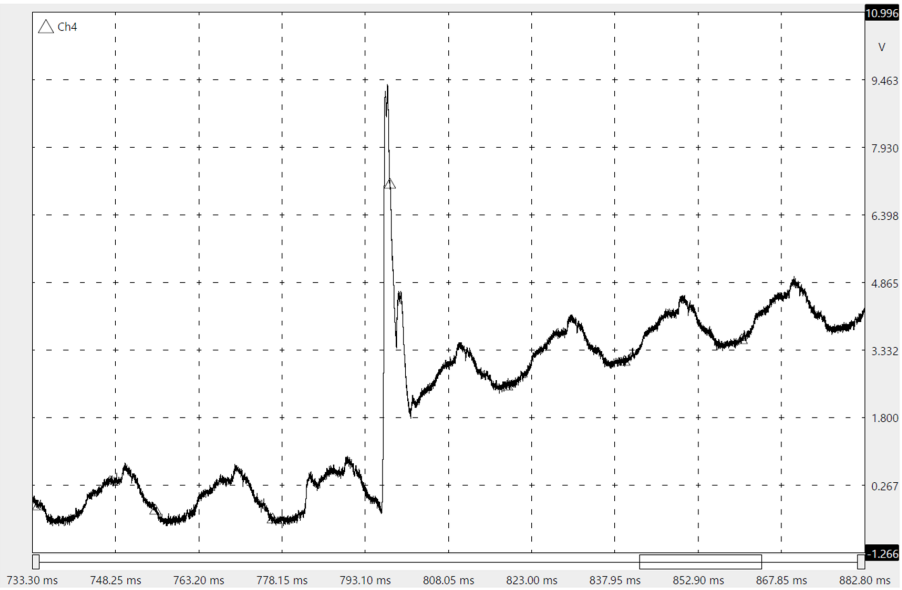

Figure 2. Inrush current on the positive HV+ line.

2.1.1 Subsubsection

Hello, here is some text without a meaning. This text should show what a printed text will look like at this place. If you read this text, you will get no information. Really? Is there no information? Is there a difference between this text and some nonsense like “Huardest gefburn”? Kjift – not at all! A blind text like this gives you information about the selected font, how the letters are written and an impression of the look. This text should contain all letters of the alphabet and it should be written in of the original language. There is no need for special content, but the length of words should match the language.

3 Second Approach: Current-based Classification and Control

Once identified the issues with the first approach, we attempted to design a controller based on the classification suggested by Verdoold (add reference).

The strategy adopted will be to first classify the electrospray mode by looking a current values on the system, and then experimentally design a controller that can move from an intermittent to a cone-jet spray mode.

However, Verdoold's method was designed for the single nozzle, and it is not clear if we can extend his classification to a multinozzle configuration. Therefore, part of this work includes an attempt to extend his classification to the system developd by Gilbert.

3.1 Measuring the currents by spray mode

The first test done was to measure the current on all three lines of the sprayhead and verify if we see a pattern in the shape of current that can be used to classify the spray mode. Figure 3 shows the setup used for this test.

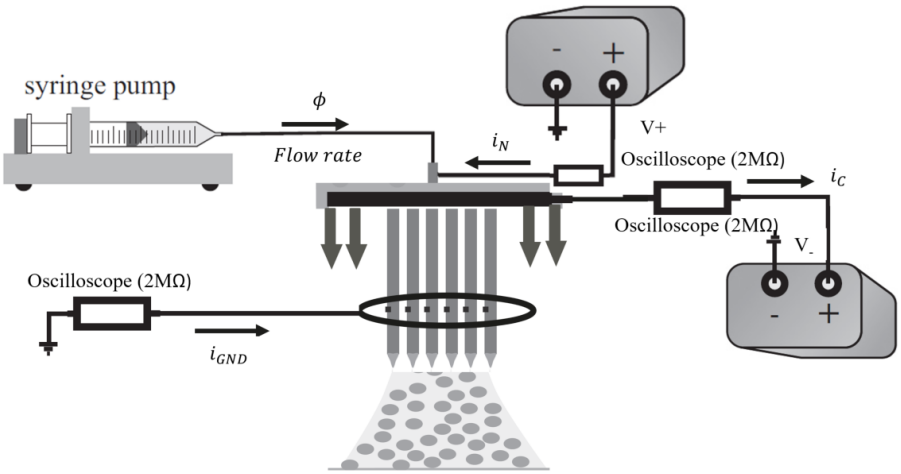

Figure 3. Setup to measure all three currents on the sprayhead.

Using three oscilloscopes, all three currents were sampled at 5 kHz, collecting 20.000 samples of each (totalling a 4 seconds time window). Notice that, although the oscilloscope has multiple channels, we cannot use the same oscilloscope as the channels are interconnected internally: the high voltage differences would damage the instrument. Therefore, we use one oscilloscope for each line.

Figure 4 shows the waveforms obtained for $\phi = 20\,\text{mL/h}$.

As we can see in Figure 4, we don't see a clear distinction in the shape of the current by different spray modes, in both time windows. We repeated the test for $\phi = 30\,\text{mL/h}$ and $\phi = 50\,\text{mL/h}$, obtaining the same result, as shown in Figure 5

Figure 4. i_N, i_{GND} and i_C by different spray modes.

Figure 5. i_N, i_{GND} and i_C by different spray modes for all ϕ.

Without a clear distinction in the current waveforms it is not possible to continue with this approach. Therefore, we need to first understand why we are not seing distinctions in the shape of the current, particularly between the intermittent and cone-jet spray modes, as it is clear in the literature that there should be a difference.

To do this, we'll begin by attempting to reproduce Verdoolds results, with the goal of isolating if the problem is our measurement strategy or if it is something related to the sprayhead itself.

3.2 Reproducing Verdoold's Results

Figure 6 shows the setup used to reproduce Verdoolds approach. We used a sampling frequency of 5 kHz and $\phi = 1\,\mathrm{mL/h}$.

Figure 6. Setup used to reproduce Verdoold's classification method.

The results obtained are shown in Figure 7.

Figure 7. Setup used to reproduce Verdoold's classification method.

As we can see in Figure 7, we see a clear distinction between the spray modes, which is what we wish to see in the multinozzle. We can conclude that our measurement methodology can reproduce the results, therefore it must be something in the multinozzle that is "hiding" the intermittent spray signal.

Comparing the single nozzle setup on Figure 6 and the multinozzle on Figure 3, the most significant difference is indeed the presence of the crown. Therefore, let's begin by understand the influence of the crown on i_{GND}, which is the current that we know is capable of showing a distinction of spraying modes.

3.3 Crown influences on i_{GND}

To understad the influence of the crown on the ground current, we'll use the same setup shown on Figure 3, but we'll make $V_+ = 0\,\text{V}$, $\phi = 0\,\text{mL/h}$ and measure i_{GND} for different crown voltages. Since there is no flow and no positive voltage, we'll be measuring the current on the groung ring introduced by the crown only.

Figure 8 shows the shape of i_{GND} for different values of V_-.

Figure 8. i_{GND} for different values of V_-. (a) Waveform and (b) standard deviation

As seen of Figure 8 (a), the crown alone introduces a signal on i_{GND} starting from $V_- = -4\,\text{kV}$, which increases in both average value and standard deviation as V_- increases. This is consistent with was happens at the crown: from $V_- = 4\,\text{kV}$ the sharp needles of the crown begin to ionize the air, which produces that ions that can be directed to ground ring. This results in a current $i_{GND} > 0$ induced by the crown.

In addition, on Figure 8 (b) we see that the standard deviation introduces by the crown is significant. As we saw on Figure 7, the intermittent spray mode presents peaks in the current signal in order of 100 nA, but the "noise" introduced by the crown alone is already over 50 nA. Therefore, it is reasonable to assuem that the reason we are not seing a good distinction between the spray modes on Figure 4 is because of this signal introduced by the crown.

3.3.1 Atenuating Crown Influences on i_{GND}

In order to verify the above hypothesis, we can try to reduce the influence of the crown in the signal and verify if the intermittent signal becomes distinguishable. We can achieve this in two ways:

- Reduce crown voltage
- Add filters in the signal

As we saw in Figure 8 (a), the smaller V_{-}, the smaller the introduced noise in i_{GND}. Then, we can redo the measurements with a smaller crown voltage.

In addition, we can add digital filters in the oscilloscope to remove the following unwanted frequencies:

- 50 Hz frequency from the electric grid: use a stop band in the range 48 - 52 Hz
- All frequencies above 100 Hz: use low pass filter with cut-off frequency 100 Hz.

Note that, as shown by Verdoold, the intermittent peaks are usually under 100 Hz. Therefore, we can remove anything above this frequency from the signal as it is not what we wish to measure.

Using this, we get ...

3.3.2 8 vs 16 Needle in the Crown

3.4 Optimizing the Signal Acquisition

In the previous sections, the signal was acquired using the minimum sampling frequency suggested by the Verdoold of $f_s = 5\,\text{kHz}$. A sample size of $N_s = 20.000$ was used to obtain a spectral resolution of 0.25 Hz for frequency domain anaysis, also suggested by Verdoold as the minimum. However, talks with Gilbert showed that the sampling frequency was too computationally expensive and the sample size was too slow, as it resulted in a sampling time window of 4 seconds, which is too large.

Therefore, to attempt to meet these requirements, we need to find the minimum sampling frequency and minimum sample size that can still reliably distinguish the signal of the intermittent from the cone-jet.

To do this, we'll use the following method:

- Collect a time window of $T = 100$ seconds for different values of f_s, resulting in a sample size of $N_s = T \cdot f_s$

- Break the $T = 100$ seconds into smaller time windows - denoted as S_i - of size T_S.
- Calculate the relevant statistical parameters in each S_i and store these values in an array of size T/T_S
- Plot a boxplot of the calculated statistical parameters

Figure 9 further explains the method above visually. T_S will be chosen for different values for the result to be verified. Note that $i = 1, 2, ..., T/T_S$, and the goal is to find the minimum T_S.

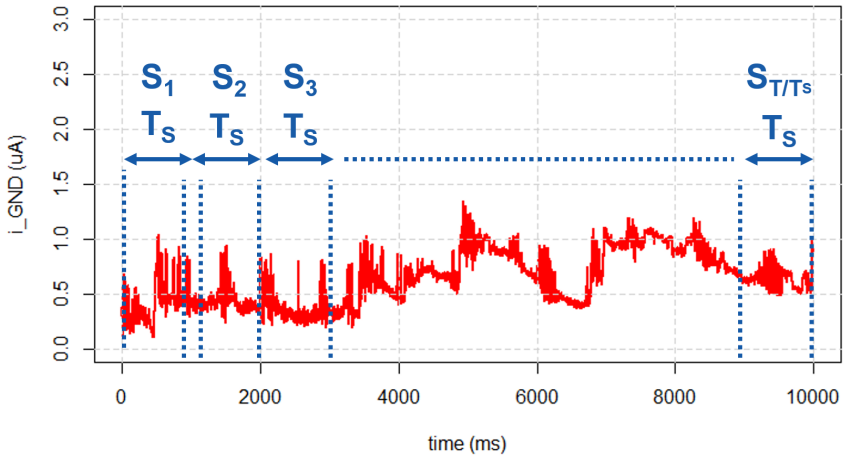

Figure 9. Method to find the minimum sample size that can still classify the EHDA mode via the current.

We'll use the same setup shown in Figure 3, using only the oscilloscope for i_{GND}. We begin with $f_s = 5\,\text{kHz}$, with $T_S = 0.01\,\text{s}; 0.1\,\text{s}; 1\,\text{s}; 10\,\text{s}$. Note that we are first changing T_S over four orders of magnitude to understand the general influence of T_S on the calcualated standard deviation. The result obtained is shown on Figure 10.

As we can see on Figure 3, $T_S = 1\,\text{s}$ appears to be the best sample size to differentiate between the intermittent and the cone-jet. Other orders of magnitude of T_S do not allow for a clear distinction between spraying mode via the statistical values. The next test is to change T_S around 1 second and compare them, using $T_S = 0.25\,\text{s}; 0.5\,\text{s}; 0.75\,\text{s}; 1\,\text{s}$. Figure 3 shows the results obtained for this test.

As seen on Figure 11, T_S appears to be the smallest sample size that can differentiate the spraying modes.

Now we need to find the minimum sampling frequency that can distinguish the spraying modes. We'll fix $T_S = 0.5\,\text{s}$ and compare the calculated statistical parameters for the following values of f_s: $f_s = 0.5\,\text{kHz}; 1\,\text{kHz}; 2\,\text{kHz}; 5\,\text{kHz}$. Figure 12 shows the result obtained for this test.

As we can see on Figure 12, $f_s = 2\,\text{kHz}$ appears to the be the smallest sampling frequency that can still distinguish the spraying modes.

The conclusion we can derive from these tests is that $T_S = 0.5\,\text{s}$ and $f_s = 2\,\text{kHz}$ are the mininum sample size and sampling frequency that can distinguish the spraying

Figure 10. Result for the first test.

Figure 11. Result for the second test.

modes via statistical parameters. Note that this results in a sample size of $N_s = T_S f_s = 1.000$, which uses significantly less memory than the $N_s = 20.000$ suggested by Verdoold. We'll move forward with these values of N_s and f_s, seeking to test the classification with parameters that are consistent with Gilbert's requirements.

Figure 12. Result for the second test.

3.5 Optimizing the Classification

3.5.1 Trying different statistical parameters

So far, we've only the standard deviation of the signal to differentiate the spraying modes. However, we can also use other statistical parameters to distinguish the waveforms. The first one that we can try is the Relative Standard Deviation (RSD), defined on Equation 1

$$RSD = \left| \frac{\sigma}{\overline{I}} \right| \tag{1}$$

where

- σ: standard deviation
- $\overline{I}$: arithmetic mean

Table 1 shows how the RSD can be a useful metric in the classification. When the spraying mode is intermittent, we expect the signal to display a large σ and a small $\overline{I}$, since the potential is lower and therefore also the mean value of the current in the system. This results in an overall value large value of the ratio.

On the other hand, when we have a cone-jet, we expect the signal to display a small σ - as the signal is much more stable - and a larger $\overline{I}$, given the larger potential. This results in an overall value small value of the ratio.

Therefore, both components of the fraction contribute in opposite directions to change the overall value of the ratio between the spraying modes. IMPROVE THIS.

Table 1. Expected behaviour of RSD for different spraying modes.

	Intermittent	**Cone-jet**
Numerator (σ)	HIGH	LOW
Denominator ($\overline{I}$)	LOW	HIGH
Overall Ratio ($\sigma/\overline{I}$)	LARGE	SMALL

Figure 13 shows the the same result of Figure 12 using the RSD instead of the standard deviation.

Figure 13. Result for the second test.

As we can see on Figure 13, we can achieve a good distinction between the spraying modes with the RSD. However, the order of magnitude of the value is very small, which can be inconvenient. A simple to resolve this is take the inverse of the RSD, that we can define as the Signal-to-Noise Ratio (SNR), shown on Equation 2

$$SNR = \frac{1}{RSD} = \left|\frac{\overline{I}}{\sigma}\right| \tag{2}$$

In Equation 2, we call the standard deviation as the "noise", and the mean as the "signal". Figure 14 shows the same result of Figure 12 using the SNR.

WRITE CONCLUSION OF THIS SECTION

3.5.2 Classification via small Neural Networks

ASK BEN

Figure 14. Result for the second test.

3.6 Proof-of-Concept Real-time EHDA Classification

Figure 15. The SAP data model based on an UML class diagram: classes and relationships.

TODO

- try to reduce sample window
- use subsequent windows
- show commmon issues (step in the current value, etc)
- add pseudocode + complexity

3.7 Proof-of-Concept Real-Time EHDA Control

TODO

- problem wth subsequent window: how will it take into account the adjusts we're making:
- is it fast enough? if it even works at all!
- add pseudocode + complexity

References

Carrasco-Munoz, A., Barbero-Colmenar, E., Bodnár, E., Grifoll, J., and Rosell-Llompart, J. (2022). Monodisperse droplets and particles by efficient neutralization of electrosprays. *Journal of Aerosol Science*, 160:105909.